ELECTRONIC SUPPLEMENTARY INFORMATION

From droplets to ions: A comprehensive and consecutive ion formation modelling in atmosphere pressure interface of electrospray ionization mass spectrometry

*He Xingliang, Wang Xu, Guo Xing, Wu Mengfan, Deng Fulong, Zeng Pengyu, Zhao Zhongjun, * and Duan Yixiang**

Research Center of Analytical Instrumentation, School of Mechanical Engineering, Sichuan University

1. Details of the background fields simulation

1.1 Physical system

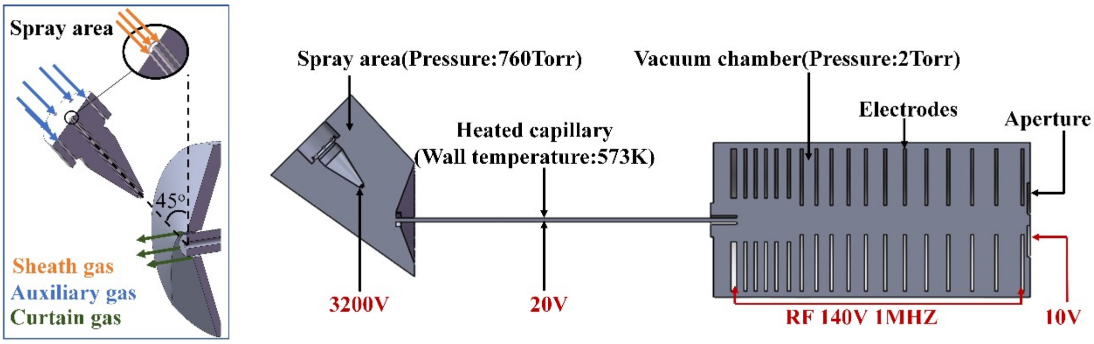

Fig.S1 The physical system

The physical system applied in our work is shown in Fig.S1, as also described in the manuscript file, the system is composed by an atmospheric spray area (pressure at 760 torr), a heated transfer capillary and a vacuum chamber (pressure at 2 torr). The axis of the ESI tip in the spray area is not aligned with the inlet of the transfer capillary but at an angle (45 degree in our model) to it. In addition, the distance between the ESI tip and the inlet of the capillary is often in the range of 10-20 mm[1]. In practice, this distance will influence the intensity of the electrical field and the transmission efficiency of the ions, which is fixed at 10 mm in this simulation. There are three gas inflows in the spray area: sheath gas, auxiliary gas and curtain gas. Generally, the sheath gas is utilized to enhance the transmission efficiency by minimizing the radial dimension of the ESI plume and aid the droplet atomization. The auxiliary gas, curtain gas and the transfer capillary (Length: 60.27 mm, Outer diameter: 1.56 mm, Inner diameter: 0.7 mm) needs to be heated, because they are deployed to benefit the evaporation and desolvation. Given the huge pressure difference between the inlet and outlet of the transfer capillary, a supersonic expansion[1] will be formed in the vacuum chamber. Therefore, in the vacuum chamber, the progressively spaced stacked ring ion guide[2] is applied to reduce ion loss. The ion guide is composed of 18 toroidal electrodes with uniform width (0.5 mm). The gaps between these electrodes (from capillary to aperture) are 1.3 mm, 1.3 mm, 1.3 mm, 1.35 mm, 1.7 mm, 1.75 mm, 2.1 mm, 2.15 mm, 2.5 mm, 2.55 mm, 2.9 mm, 2.95 mm, 3.3 mm, 3.35 mm, 3.7 mm, 3.75 mm, and 4.1 mm. The gap between the last electrode and the aperture is 0.6 mm. In addition, the inner radiuses of electrodes 1-6 and 7-18 are 3.85 mm and 2.58 mm, respectively. Following the ion guide is an aperture (2 mm in diameter and 0.5 mm in length) that leads to another vacuum chamber.

1.2 Electrical field simulation

After an optimization of the electrical parameters of the system through pre-experiment, the boundary condition applied in our simulation is decided. As shown in Fig.S1, during the electrical field simulation, the electrostatic potential of the ESI tip, the transfer capillary and the aperture is set as 3200 V, 50 V, and 25 V. In addition, an alternating current with 140 V amplitude (peak-to-peak value, offset at 35 V) and 1 MHz frequency is applied to the electrodes of the RF ion guide. The spatial distribution of the electrostatic potential is shown in Fig.S2 (a). For the RF field, the RF voltages of adverse phases are applied to the adjacent electrodes in the ion guide, and a pseudopotential wall can be formed and represented as[2]:

$$U_{ps} = \frac{qE^2}{4m\omega^2} \tag{S1}$$

Where E is the electrical field, q is the ion charge, m is the ion mass and ω is the frequency of the RF voltage. With the target analyte set as the protonated reserpine (m/z 609.28), the spatial distribution of the pseudopotential is calculated and shown in Fig.S2(b).

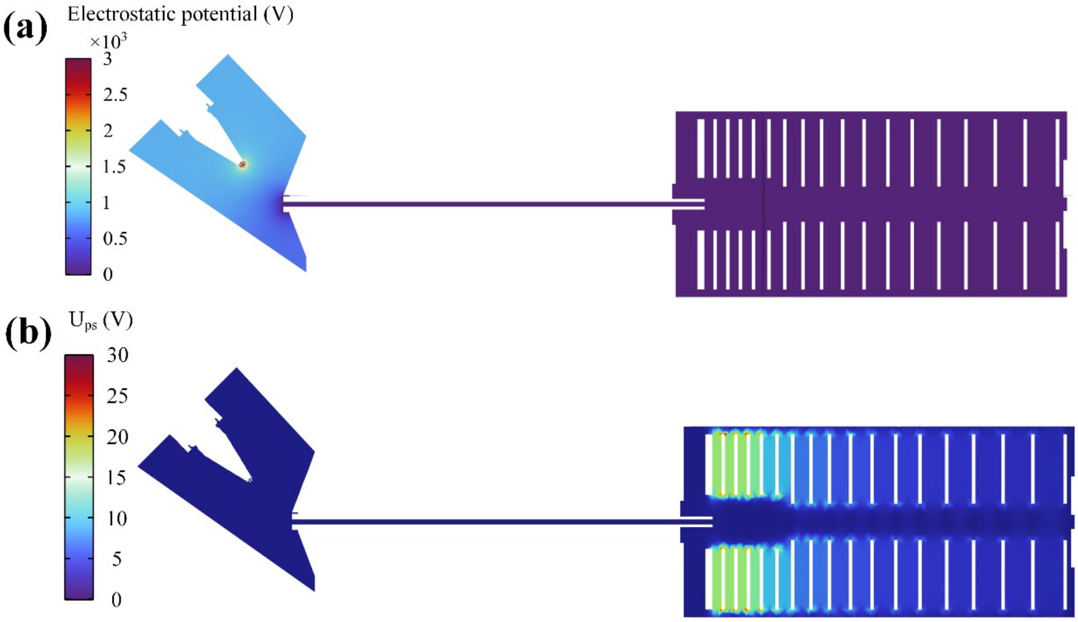

Fig.S2 The spatial distribution of (a) the electrostatic potential and (b) the pseudopotential (U_{ps}) formed by the RF ion guide

1.3 Fluid field simulation

1.3.1 Boundary conditions

There are three inflow boundaries in the physical system: the sheath gas inlet, the auxiliary gas inlet, and the curtain gas inlet. At these boundaries, the gas velocity is assumed normal to the surfaces and the magnitude is given as:0-70 m/s for the sheath gas, 20 m/s for the auxiliary gas and curtain gas. Besides, the gas temperature of these boundaries is set as: 300 K for the sheath gas, 343 K for the auxiliary gas and 573 K for the curtain gas. A backpressure imposition is applied at spray area outflow boundaries (760 torr) and the vacuum chamber outflow boundaries (2 torr). Then the maximum Knudsen number[3] of the flow area of interest (different from the particle Kn mentioned in the manuscript) can be estimated, which is around 0.001. It indicates that the gas flow can be still regard as continuum in our simulation. Then, all surfaces of the ESI-tip, the skimmer cone, the transfer capillary and the electrodes are set as isothermal no-slip walls, in which the wall temperature of the ESI-tip, the skimmer cone and the transfer capillary are given and set as 343 K, 573 K, and 573 K.

1.3.2 Models

In this simulation, a compressible gas model of air with viscosity specified by the Sutherland law was used (the impact of real gas effects on the other properties for the temperatures under consideration is negligible). Then, the Reynolds number of the gas inlets are estimated, which is 800 (sheath gas speed 70 m/s), 200, and 400 for the sheath gas, the auxiliary gas, and the curtain gas. In our work, the 2-equation turbulent Reynolds averaged Navier-Stokes model, k-ω SST model[4], is applied and the turbulence intensity of the gas inlets are set according to the estimated Reynolds number. Besides, since the velocity and compressibility of flow will change greatly in a limited spatial scale, a density-based solver[3] of Fluent is adopted. To enhance the convergence speed of the computing, the second order upwind discretization scheme[3] is applied for the flow property interpolation. The convergence criteria are set as: 1. The iterative residuals less than 1×10^{-3}. 2. The fluctuation of the maximum gas speed of the system less than 1×10^{-6}. 3. The absolute value of the sum of mass and energy fluxes of the system is less than 1×10^{-6}(normalized).

1.3.3 Mesh

A hybrid mesh of polyhedral and hexahedral elements established by Ansys Fluent (ver. 2022 R1, Cecil Township, PA) is applied in the CFD simulation, as shown in Fig.S3. In the mesh generation process, the boundary layer grid and division of grid partition method is adopted. The global maximum cell length is set below 0.5 mm. The cell length of the areas where large velocity gradients may occur is set below 0.1 mm. In addition, the grid near the electric spray plume area and air inlet is also densified. After a mesh independence verification, the total number of mesh cells are fixed as 2276081 with orthogonal quality higher than 0.2.

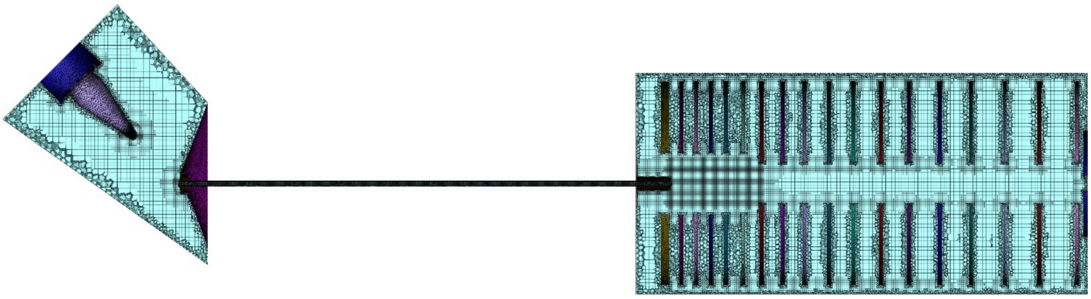

Fig.S3 The mesh used in the fluid simulation

2. Details of the particle tracing simulation

2.1 Theory of the particle tracing simulation

When the ESI ion source is operated in positive mode, an electrostatic potential difference of several kilovolts is maintained between the ESI tip and the MS inlet. At this point, an intensive electrical field appears at the ESI tip and the meniscus takes the form of a cone whose tip emits a thin jet that breaks into electrically charged drops at some distance away from the meniscus by varicose wave instabilities. And as reported in[5], when the electrospray is operated at cone-jet mode that keeps the ion source in a stable working status, it is believed that the majority of these droplets are conforms to a monodisperse size distribution. This basic fact indicates that it is sensible to specify a constant initial diameter for all the droplets released at the liquid jet (nominated as primary droplets) in the simulation. The mean radius of these initial droplets can be estimated by the scaling law[5]. For the fluids with relative permittivity (ε_r) in the range

$$12.5 \le \varepsilon_r \le 182.4 \tag{S2}$$

The initial droplets can be estimated using

$$D_d = (10.87\varepsilon_r^{-5/6} + 4.08\varepsilon_r^{-1/3})\left(\frac{Q\varepsilon_0\varepsilon_r}{K}\right)^{1/3} \tag{S3}$$

In which D_d is the diameter of the initial droplets, Q is the volumetric flow rate of the fluid, K is the conductivity of the fluid and ε_0 is the permittivity of vacuum. By assuming the droplets are released in even time interval and are shaped in spere, the time interval between each release event in our simulation can then be calculated as

$$\Delta t = \frac{4\pi(D_d/2)^3}{3Q} \tag{S4}$$

Once a primary droplet is issued, it will be entrained in gas flow and the droplet motion can be described by the Lagrangian equation

$$m_p\frac{d\vec{v}}{dt}=F_D+F_E+F_O \tag{S5}$$

In which $\vec{v}$ is the velocity vector of the droplet, m_p is the mass of the droplet, F_D is the drag force imposed by the flow field, F_E is the electrical force and F_O represents other forces (such as the Brownian force, virtual mass force and etc.). In the equation above: F_O is generally insignificant in the particle motion and can be omitted [6]. F_D is calculated using a stokes drag law modified for micron-size droplets, which will be clarified in the section below. F_E can be represented as

$$F_E=q\vec{E}+\frac{1}{4\pi\varepsilon_0}\sum_{i=1}^{n}\frac{qq_i(\vec{r}+\vec{r}_i)}{\left|\vec{r}-\vec{r}_i\right|^3} \tag{S6}$$

The electrical force of a single droplet is contributed by two terms. The first term on the right side of the equation represents the force imposed by the static electrical field, where q is the charge of the droplet and $\vec{E}$ is the intensity vector of the field. The second term is the explicit form of the Coulomb repulsion induced by the charged droplets (also known as the space charge effect) and is critical in the formation of ESI plume morphology. In this term, $\vec{r}$ is the position vector of the droplet, $\vec{r}_i$ and $\vec{q}_i$ are the position vector and charge of another droplet and n is the total number of the droplets. Except for the explicit method, the Coulomb repulsion can also be calculated in an implicit form by the PIC[6](particle in cell) method based on Poisson equation. In this method, the contribution of every charged particle to the overall electrostatic field of the system will be counted at each time step, which can be described as the equations below

$$\begin{cases}\nabla^2\phi=-\dfrac{\rho_e}{\varepsilon_0}\\ \vec{E}=-\nabla\phi\end{cases} \tag{S7}$$

Where ϕ is the potential of the electrical field and ρ_e is the space charge density induced by the charged droplets. When eq (S6) is utilized, n times calculations are required for each charged droplet at every time step. Whereas the number of charged droplets within a fully-developed electrospray plume can be enormous due to the multiple fission events, the calculation of the space charge effect using the equation above may turned to be difficult with common computing power. And when eq (S7) is applied instead, the space charge effect can be simply evaluated by the calculating effective electrical field which contains the distortion caused by all the charged liquid droplets. The advantage of the PIC method will become increasingly significant with the growth of the number of droplets and thus is applied in our model.

In our simulation, the evaporation of droplets is established using the classic Stefan-Fuchs model[7] in continuum regime, which cover the effects of the convective heating and the advective transport of the vapor-gas mixture

$$\begin{cases}\dfrac{dm_p}{dt}=-2\pi d_p\dfrac{k_r}{C_{p,r}}\log(1+B_M)\\ Q=\dfrac{dm_p}{dt}h_p(\dfrac{B_T}{B_M}-1)\\ m_pC_p\dfrac{dT}{dt}=Q\end{cases} \tag{S8}$$

In the above equations, the reference specific heat capacity ($C_{p,r}$), reference thermal conductivity (k_r), Spalding mass transfer number (B_M) and Spalding thermal transfer number (B_T) can be further represented as

$$
\begin{aligned}
C_{p,r} &= Y_{v,r} C_{p,v}(T_r) + (1 - Y_{v,r}) C_p(T_r) \\
k_r &= Y_{v,r} k_v(T_r) + (1 - Y_{v,r}) k(T_r) \\
B_M &= \frac{Y_{v,s} - Y_{v,a}}{1 - Y_{v,s}} \\
B_T &= \frac{C_{p,r}(T_f - T)}{h_p} \\
T_r &= \frac{2}{3} T_f + \frac{1}{3} T \\
Y_{v,r} &= \frac{2}{3} Y_{v,s} + \frac{1}{3} Y_{v,a} \\
Y_{v,s} &= \left[1 + \left(\frac{p}{p_{v,s}} - 1 \right) \frac{M_f}{M_v} \right]^{-1} \\
Y_{v,a} &= \left[1 + \left(\frac{p}{p_{v,a}} - 1 \right) \frac{M_f}{M_v} \right]^{-1} \\
p_{v,s} &= p_{v,ref} \exp\left[-\frac{h_p M_v}{R} \left(\frac{1}{T} - \frac{1}{T_{ref}} \right) \right]
\end{aligned}
\tag{S9}
$$

In the above equations: $Y_{v,r}$ is the reference mass fraction of vapor; $Y_{v,s}$is the mass fraction of vapor on the droplet surface; $Y_{v,a}$is the mass fraction of vapor in fluid; T_r is the reference temperature; T_s is the fluid temperature; T_{ref} is the reference temperature; $C_{p,v}$is the specific heat capacity of vapor; k_v and k are the thermal conductivity of vapor and solvent; M_f and M_v are the molecular weight of fluid and vapor; p is the environmental pressure; $p_{v,s}$is the saturated vapor pressure on droplet surface; $p_{v,a}$is the environmental saturated vapor pressure; $p_{v,ref}$ is the saturated vapor pressure at reference temperature; R is the ideal gas constant (8.314 [J/(mol·K)]). In the above parameters,$C_{p,v}$, C_p, h_p, k_v, k, M_f, and M_v are the thermodynamic properties of the solution and need be input into the model.

With the evaporation goes on, the Coulomb repulsion generated by the charge inside the droplet gradually approaches its surface tension, and when d_p lower to a certain value d_R (the Rayleigh limit[8]), the droplet disrupts and release several progeny droplets

$$
d_R = \left(\frac{8\pi^2 \varepsilon_0 \gamma}{q^2}\right)^{\frac{1}{3}} \tag{S10}
$$

The mass and charge of the droplet after the fission event, d_p' and q' can be described as

$$
\begin{cases}
d_p' = d_p (1 - l_m)^3 \\
q' = q(1 - l_q)
\end{cases}
\tag{S11}
$$

In which l_m and l_q are the loss rates of the mass and charge of the primary droplets. According to[8], the values of l_m and l_q are set as 0.02 and 0.15 in this simulation. With regard to the progeny droplets, the diameter ($d_p^{\,p}$) and number produced in a fission event (N) can be represented as

$$
\begin{cases}
d_p^{\,p} = \frac{1}{8} d_R \\
N = l_m \left(\frac{d_R}{d_p^{\,p}}\right)^3 \approx 10
\end{cases}
\tag{S12}
$$

It should be noted that the mass loss of the primary droplet (2%) is much less than its charge loss (15%), which indicates that the charge density of a progeny droplet is almost 7.7 times of its primary droplet. These highly-charged progeny droplets are perfect candidates of the gas phase ions that can be analysed. Then, as illustrated in the manuscript, when the particle Knudsen number for a droplet is greater than 0.1, the evaporation stops and the droplet converts to a solvent cluster or ion cluster. Even if this simplification can bring in errors in the estimation of the evolution of a single droplet, the results of the whole charged plume can still be instructive in a statistical manner. The clusters are then counted at the outlet of the transfer capillary. According to the counted results, the ions are then reemitted in the vacuum chamber, where the fluid-particle interaction is determined by the collision model.

2.2 The drag force model of droplets-fluid interaction

Generally, the drag force model can be represented as[7]

$$F_D = \frac{1}{\tau_p} m_p u' \tag{S13}$$

in which τ_p is the particle velocity response time, u' is the relative speed between the particle and the flow field. The expression of τ_p is changeable according to different circumstances, which can be determined by the relative Reynolds number

$$\mathrm{Re}_R = \frac{\rho |u'| d_p}{\mu} \tag{S14}$$

where ρ is the density of the fluid, μ is the viscosity of the fluid and d_p is the diameter of the droplet. According to the simulation results, the range of Re_R can be roughly estimated by assuming

$$\begin{aligned} |u'| &= 0.1\text{-}300 \text{ [m/s]} \\ d_p &= 0.1\text{-}5 \text{ [}\mu\text{m]} \end{aligned} \tag{S15}$$

In this case, the Re_R value in the spray zone is between 2.72×10^{-7} and 98.62. In this case, the Schiller-Neumann model (for $Re_R < 800$) [7] is appropriate, such that

$$\tau_p = \frac{\rho_p d_p^{\,2}}{18\mu(1 + 0.15\mathrm{Re}_R^{\,0.687})} \tag{S16}$$

Where ρ_p is the density of the droplet. The drag law above is feasible when the fluid surrounding each particle can be treated as continuum. When the gas density is extremely low or the particle size is very small, the assumption breaks down and the rarefaction effect should be included. The rarefaction effect can be quantified by the particle Knudsen number

$$Kn = \sqrt{\frac{\pi}{2p\rho}} \frac{\mu}{d_p} \tag{S17}$$

Only when $Kn = 1$, the surrounding fluid of particle is continuum. With the assumption shown in eq (S15), the Kn in the spray area distributes between 1.81×10^{-4} and 2.56×10^{-4}, thus the rarefaction effect can be omitted and the drag force model in the particle tracing simulation can be derived as

$$F_D = \frac{18\mu m_p u'(1 + 0.15\mathrm{Re}_R^{\,0.687})}{\rho_p d_p^{\,2}} \tag{S18}$$

However, for droplets insides the transfer capillary (where the pressure is as low as 252 torr), the maximum Kn is around 5. In this situation, a slip correction must be applied to the τ_p. And in our work, the Cunningham-Millikan-Davies (CMD) model[7] is utilized

$$\tau_p' = \frac{\tau_p}{1 + Kn(C_1 + C_2 e^{-\frac{C_3}{Kn}})} \tag{S19}$$

Where τ_p' is the corrected respond time and the value of C_1, C_2, and C_3 are given as 2.514, 0.8, and 0.55.[7]

2.3 The thermodynamic properties of charged droplets

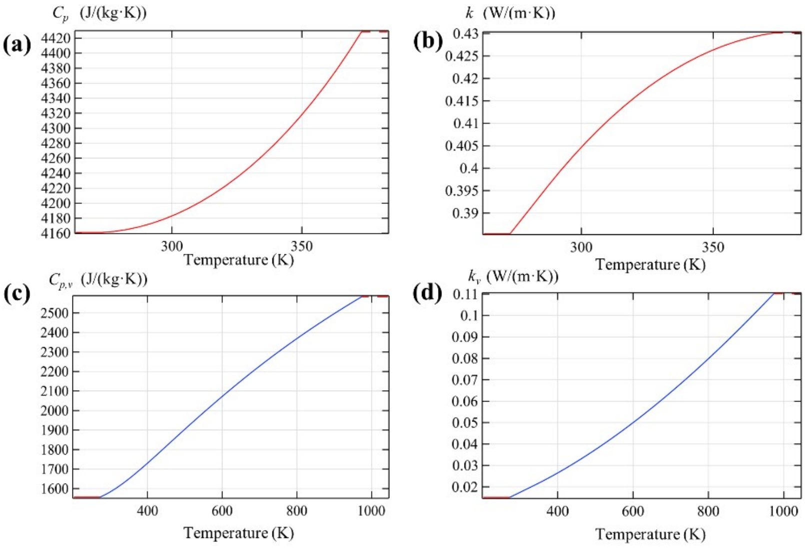

Figure S4. The curves of (a) C_p, (b)k, (c)$C_{p,v}$, and (d) k_v

In our simulation, the mixture of water and methanol (50:50) is applied as the solvent, and the relevant thermodynamic properties are solved using the COMSOL module of thermodynamic properties estimation. Among these parameters, the values of C_p,k,$C_{p,v}$, and k_v are depend on temperature, which are shown in Fig.S4(a-d). Besides, according to the estimated results, the values of h_p, M_f, and M_v are 1249.35[kJ/kg], 28.97 [g/mol], and 23.06 [g/mol].

2.4 The time step applied in the particle tracing

As introduced before, the particle tracing module is generally consisted by two independent parts: 1. The droplet evolution model. 2. The ion optics model. Since the fluid interaction mechanism is different for these two models, the time scale of these two models can be quite different. In both methods, the calculation is proceeded using the built-in transient solver of COMSOL Multiphysics, in which the time step is chosen automatically but no bigger than a given maximum value. The maximum time step for the droplet evolution model is correlated to the particle velocity response time. And the maximum time step for the ion optics is related to the mean free path and the speed of ions. The maximum time step for both model is then decided by time step independence verification, which is 1×10^{-7} s and 1×10^{-8} s.

Reference

1 J. H. Gross, *Mass spectrometry: a textbook*, Springer Science & Business Media, 2006.
2 R. T. Kelly, A. V. Tolmachev, J. S. Page, K. Tang and R. D. Smith, *Mass Spectrom Rev*, 2010, **29**, 294-312.
3 R. D. Zucker and O. Biblarz, *Fundamentals of gas dynamics*, John Wiley & Sons, 2019.
4 Menter F R*, Improved two-equation k-omega turbulence models for aerodynamic flows*,1992.
5 J. Rosell-Llompart, J. Grifoll and I. G. Loscertales, *Journal of Aerosol Science*, 2018, **125**, 2-31.
6 W. Wang, S. Bajic, B. John and D. R. Emerson, *J Am Soc Mass Spectrom*, 2018, **29**, 600-612.
7 S. Basu, A. K. Agarwal, A. Mukhopadhyay and C. Patel, *Droplets and sprays: applications for combustion and propulsion*, Springer, 2017.
8 C. J. Hogan Jr and P. Biswas, *Journal of the American Society for Mass Spectrometry*, 2008, **19**, 1098-1107.